Higher order baryon number fluctuations at finite temperature and density

Wei-jie Fu,[1] Xiaofeng Luo,[2] Jan M. Pawlowski,[3,4] Fabian Rennecke,[5] Nu Xu,[6,7] and Shi Yin[1]

[1] *School of Physics, Dalian University of Technology, Dalian, 116024, P.R. China*
[2] *Key Laboratory of Quark & Lepton Physics (MOE) and Institute of Particle Physics, Central China Normal University, Wuhan 430079, China*
[3] *Institut für Theoretische Physik, Universität Heidelberg, Philosophenweg 16, 69120 Heidelberg, Germany*
[4] *ExtreMe Matter Institute EMMI, GSI, Planckstraße 1, D-64291 Darmstadt, Germany*
[5] *Physics Department, Brookhaven National Laboratory, Upton, NY 11973, USA*
[6] *Lawrence Berkeley National Laboratory, Berkeley, CA 94720, USA*
[7] *Institute of Modern Physics of CAS, Lanzhou 730000, China*

We study the generalized susceptibilities from kurtosis which is known as the χ_4^B/χ_2^B to the χ_8^B/χ_2^B. The results are obtained under the finite temperature and baryon density. We give the comparison of our results with the lattice QCD results under the vanishing μ_B. We get the numerical results under the Polyakov-quark-meson (PQM) model with the functional renormalisation group (FRG) approch.

PACS numbers: 11.30.Rd, 11.10.Wx, 05.10.Cc, 12.38.Mh

I. INTRODUCTION

We ...

II. LOW ENERGY EFFECTIVE MODEL UNDER FRG APPROACH

Here we perform our calculation under the Polyakov loop improved quark-meson model. The effective action which is depend on the evolution of the infrared cutoff scale is

$$\Gamma_k[\Phi] = \int_x \Big\{ Z_{\psi,k}\bar{\psi}\Big[\partial\!\!\!/ - \gamma_0(igA_0+\hat{\mu})\Big]\psi + \frac{1}{2}Z_{\phi,k}(\partial_\mu\phi)^2 + h_k\bar{\psi}\big(T^0\sigma + i\gamma_5 T^i\pi^i\big)\psi + U_k(\rho) - c\sigma\Big\}. \quad (1)$$

In this work we consider the light quark only, e.g. u quark and d quark, so we have $N_f = 2$. For $2+1$ flavor low energy effective model see, e.g., [1]. The value of index $\mu = 0,1,2,3$ and $i = 1,2,3$. The integral sign stands for the intergral of the temporal and spatial components, e.g. $\int_x = \int_0^\beta \int d^3x$. The β is the temporal length in the finite temperature field theory $\beta = 1/T$. The superfield contain all kind of fields $\Phi = (\psi, \bar{\psi}, \phi)$. $\psi = (u, d)$ is the fermion field and $\bar{\psi}$ is the corresponding anti-fermion field. The $O(4)$ invariant effective potential $U_k(\rho)$ is related to the meson field $\phi = (\sigma, \pi^i)$ with $\rho = \phi^2/2$. The $c\sigma$ is the chiral symmetry breaking term. The generators of the $SU(N_f)$ flavor space is give by T^0 and T^i which obey the rules:$T^0 = 1/\sqrt{2N_f}\mathbb{1}_{N_f\times N_f}$ and $\mathrm{Tr}(T^iT^j) = 1/2\delta^{ij}$. $Z_{\psi,k}$ and $Z_{\phi,k}$ are the wave function renormalisations of the quark and meson fields and h_k is the running Yukawa coupling. $\hat{\mu}$ is the quark chemical potential matrix, and we have $\mu_B = 3\mu$. A_0 is the gluon background which is involved through the Polyakov loop in our calculation.

The effective action is running with a FRG scale k which is a infrared cutoff. The information of the quantum fluctuations are removed. With the k running from ultraviolet point to infrared point, the behaviour of the fluctuations can be obtained. To describ the running of the effective action with the cutoff scale k, we derive the flow equation of the effective action with the Wetterich equation, see [2]

$$\partial_t\Gamma_k[\Phi] = \frac{1}{2}\mathrm{Tr}(G_{\phi\phi,k}\partial_t R_k^\phi) - \mathrm{Tr}(G_{\psi\bar{\psi},k}\partial_t R_k^\psi). \quad (2)$$

The differential equation is related to the renormalisation group time, e.g. $t = ln(k/\Lambda)$, with the ultraviolet (UV) cutoff Λ as the initial point of the flow equation. The low energy effective model is well applied with the scale $k \lesssim 1GeV$. With the k coming to 0 in the process of solving the differential equation we get the physics value of the effective action. Then the propagators in the flow equation can be derived by the two point correlation functions

$$G_{\phi\phi/\psi\bar{\psi}}[\Phi] = \frac{1}{\Gamma_k^{(2)}[\Phi] + R_k}\bigg|_{\phi\phi/\psi\bar{\psi}}. \quad (3)$$

On the l.h.s of the flow equation is the derivation of the effective action. The analytic form of the flow equations should be calculated by the loop diagram on the r.h.s.

The core issue of the PQM model is to investigate the thermodynamical of the system which is related to the meson effective potential for the information of the chiral symmetry breaking it carries. If we only consider the flow equation of the effective potential without the flow of the wave function renormalisation and Yukawa coupling we get the result of the local potential approximation (LPA). Here we give the results of beyond LPA that we take all the quantum fluctuations into account, the running of the $Z_{\phi/\psi,k}$ and h_k are completly calculated. The meson and quark wave function renormalisations are split into $Z^{\parallel}_{\phi/\psi}$ and $Z^{\perp}_{\phi/\psi}$ for the breaking of the $O(4)$ symmetry of

the heat bath. However, the spatial components play the most significant role of the physical fluctuations, see [3], so it is reasonable to assume $Z^{\parallel}_{\phi/\psi} = Z^{\perp}_{\phi/\psi}$ in our work to simplify calculation.

Now come to the gluon part, we involve the gluon effect by the glue potential which is related to the Polyakov loop with temporal gluonic background A_0

$$L(\boldsymbol{x}) = \frac{1}{N_c}\langle \mathrm{Tr}\, \mathcal{P}(\boldsymbol{x})\rangle, \qquad \bar{L}(\boldsymbol{x}) = \frac{1}{N_c}\langle \mathrm{Tr}\, \mathcal{P}^{\dagger}(\boldsymbol{x})\rangle\,, \quad (4)$$

the Polyakov loop has the form of

$$\mathcal{P}(\boldsymbol{x}) = \mathcal{P}\exp\left(ig\int_0^{\beta} d\tau A_0(\boldsymbol{x},\tau)\right). \quad (5)$$

The glue potential which we employed in the model, see [4], is parameterized as the form below

$$\begin{aligned} U_{glue}(L,\bar{L})/T^4 =& -\frac{a(T)}{2}\bar{L}L + b(T)\ln M_H(L,\bar{L}) \\ &+ \frac{c(T)}{2}(L^3+\bar{L}^3) + d(T)(\bar{L}L)^2. \end{aligned} \quad (6)$$

$M_H(L,\bar{L})$ stands for the Haar measure which is defined as

$$M_H(L,\bar{L}) = 1 - 6\bar{L}L + 4(L^3+\bar{L}^3) - 3(\bar{L}L)^2. \quad (7)$$

Then we give the parametric form of the factors of the a, b, c, d. The factor a, c, d have the same form

$$x(T) = \frac{x_1 + x_2/t_c + x_3/t_c^2}{1 + x_4/t_c + x_5/t_c^2}, \quad (8)$$

and the form of b is

$$b(T) = b_1 t_c^{-b_4}(1 - e^{b_2/t_c^{b_3}}), \quad (9)$$

the values of the parameters are fixed by the thermodynamics and can be found at [4]. The temperature t_c is reduced temperature by $t_c = (T - T_c)/T_c$. We rescale the reduced temperature to make the glue potential accord with the Yang-Mills theory by $(t_c)_{YM} \to \alpha(t_c)_{glue}$, and $(t_c)_{glue} = (T - T_c^{glue})/T_c^{glue}$. Here we choose $\alpha = 0.7$ and $T_c^{glue} = 270\,\mathrm{MeV}$ by fitting the kurtosis of the baryon number fluctuation with the lattice results. The effect of the Polyakov loop is working on the fermion distribution function see [5].

After the preparation above we derive the flow equation of the effective potential

$$\begin{aligned} \partial_t V_k(\rho) =& \frac{k^4}{4\pi^2}\Big[\big(N_f^2-1\big) l_0^{(B,4)}(\bar{m}^2_{\pi,k}, \eta_{\phi,k}; T) \\ &+ l_0^{(B,4)}(\bar{m}^2_{\sigma,k}, \eta_{\phi,k}; T) \\ &- 4N_c N_f l_0^{(F,4)}(\bar{m}^2_{q,k}, \eta_{q,k}; T, \mu)\Big], \end{aligned} \quad (10)$$

The $l_0^{(B/F,n)}$ is the threshold function. The definitions of the meson mass and constituent light quark mass are given by

$$\bar{m}^2_{\pi,k} = \frac{V_k'(\rho)}{k^2 Z_{\phi,k}}\,, \quad (11)$$

$$\bar{m}^2_{\sigma,k} = \frac{V_k'(\rho) + 2\rho V_k''(\rho)}{k^2 Z_{\phi,k}}\,, \quad (12)$$

$$\bar{m}^2_{q,k} = \frac{h_k^2 \rho}{2k^2 Z^2_{q,k}}\,. \quad (13)$$

Under the beyond LPA truncation we adopt in our calculation, the flow equations of wave function renormalisations and Yukawa coupling should be involved. The flow equations of the meson and quark wave function renormalisations i.e. the anomalous dimensions as follows

$$\eta_{\phi,k} = -\frac{\partial_t Z_{\phi,k}}{Z_{\phi,k}}\,, \qquad \eta_{\psi,k} = -\frac{\partial_t Z_{\psi,k}}{Z_{\psi,k}}\,. \quad (14)$$

The high order quark meson scattering which leads to the field dependent of the Yukawa coupling dosen't involve in our calculation here related research see [6]. The analytical form of the anomalous dimensions and the flow of the Yukawa coupling and the threshold functions see [5].

III. THERMODYNAMICS AND BARYON NUMBER FLUCTUATION

For the purpose of calculating the thermodynamics of our system we give the definition of the thermodynamical potential density

$$\Omega[T,\mu] = U_{k=0}(\rho) - c\sigma + U_{glue}(L,\bar{L}), \quad (15)$$

it can be solved through the equation of motion $\partial_L \Omega = 0$. From the thermodynamical potential density one can obtain the pressure of the system

$$p = -\Omega[T,\mu], \quad (16)$$

then the baryon number fluctuations can also be computed through the pressure. We give the general expression of the baryon number fluctuation

$$\chi_n^B = \frac{\partial^n}{\partial(\mu_B/T)^n}\frac{p}{T^4}. \quad (17)$$

We can also express the generalized susceptibilities by the cumulants of the baryon number distributions

$$\chi_1^B = \frac{1}{VT^3}\langle N_B\rangle\,, \tag{18}$$

$$\chi_2^B = \frac{1}{VT^3}\langle (\delta N_B)^2\rangle\,, \tag{19}$$

$$\chi_3^B = \frac{1}{VT^3}\langle (\delta N_B)^3\rangle\,, \tag{20}$$

$$\chi_4^B = \frac{1}{VT^3}\big(\langle (\delta N_B)^4\rangle - 3\langle (\delta N_B)^2\rangle^2\big), \tag{21}$$

$$\chi_6^B = \frac{1}{VT^3}\big(\langle (\delta N_B)^6\rangle - 15\langle (\delta N_B)^4\rangle\langle (\delta N_B)^2\rangle - 10\langle (\delta N_B)^3\rangle^2 + 30\langle (\delta N_B)^2\rangle^3\big) \tag{22}$$

$$\chi_8^B = ????. \tag{23}$$

The angle brackets stand for the ensemble average value and $\delta N_B = N_B - \langle N_B\rangle$. To compare the results with the lattice simulation further with the experiments we consider the kurtosis $\kappa\sigma^2 = \chi_4^B/\chi_2^B$, χ_6^B/χ_2^B and χ_8^B/χ_2^B.

IV. NUMERICAL RESULTS

For the purpose of solving the flow equation of the effective potential Eq. (10) we use the Tylor expansion approach around the expansion point κ. The renormalised effective potential under the Tylor expansion is

$$\bar{U}_k(\bar{\rho}) = \sum_{n=0}^{N_u}\frac{\bar{\lambda}_{n,k}}{n!}(\bar{\rho}-\bar{\kappa}_k)^n, \tag{24}$$

with $\bar{U}_k(\bar{\rho}) = U_k(\rho)$, $\bar{\lambda}_{n,k} = \lambda_{n,k}/(Z_{\phi,k})^n$, $\bar{\rho} = Z_{\phi,k}\rho$, $\bar{\kappa}_k = Z_{\phi,k}\kappa_k$. Here we take $N_u = 5$ for the well convergence of effective potential. The running cutoff scale dependent expansion point κ_k is emploied in our numerical calculation. Then we can get the Tylor expansion flow equation from Eq. (10) and Eq. (24)

$$\partial_{\bar{\rho}}^n\Big(\partial_t|_\rho \bar{U}_k(\bar{\rho})\Big)\Big|_{\bar{\rho}=\bar{\kappa}_k} = (\partial_t - n\eta_{\phi,k})\bar{\lambda}_{n,k} - (\partial_t\bar{\kappa}_k + \eta_{\phi,k}\bar{\kappa}_k)\bar{\lambda}_{n+1,k}\,. \tag{25}$$

There is another chosen of the expansion point i.e. fixed point which the bare κ is independent on the cutoff scale which has a good convergence property of N_u, see, e.g.[3, 6]. However, the fixed point expansion may introduce temperature dependence into the Tylor expansion and the thermodynamics will be influence by this property, so we choose the running point expansion in this work. The running point is the solution of the equation of motion

$$\frac{\partial}{\partial\bar{\rho}}\Big(\bar{U}_k(\bar{\rho}) - \bar{c}_k(2\bar{\rho})^{\frac{1}{2}}\Big)\Big|_{\bar{\rho}=\bar{\kappa}_k} = 0\,. \tag{26}$$

We emphasize that the equation of motion must be satisfied under every value of the infrared cutoff. The renormalised explicit symmetry breaking term is $\bar{c}_k = c/(Z_{\phi,k})^{1/2}$, with the flow $\partial_t\bar{c}_k = (1/2)\eta_{\phi,k}\bar{c}_k$. From Eq. (25) and Eq. (26) we can obtain the flow of the renormalised running expansion point

$$\partial_t\bar{\kappa}_k = -\frac{\bar{c}_k^2}{\bar{\lambda}_{1,k}^3 + \bar{c}_k^2\bar{\lambda}_{2,k}}\Big[\partial_{\bar{\rho}}\Big(\partial_t\big|_\rho\bar{U}_k(\bar{\rho})\Big)\Big|_{\bar{\rho}=\bar{\kappa}_k} + \eta_{\phi,k}\Big(\frac{\bar{\lambda}_{1,k}}{2} + \bar{\kappa}_k\bar{\lambda}_{2,k}\Big)\Big]\,. \tag{27}$$

In this work we don't consider the field dependence of the Yukawa coupling and the renormalised Yukawa coupling is $\bar{h}_k = h_k/(Z_{\psi,k}Z_{\phi,k}^{1/2})$.

Now we give the ultraviolet of the flow equations i.e. the initial conditions of the differential equations. The ultraviolet cutoff scale is set to $\Lambda = 700\,\mathrm{MeV}$. The parameterized effective potential at UV point is

$$U_{k=\Lambda}(\rho) = \frac{\lambda_{k=\Lambda}}{2}\rho^2 + \nu_{k=\Lambda}\rho\,, \tag{28}$$

The values of the parameters in the effective potential are $\lambda_{k=\Lambda} = 11$ and $\nu_{k=\Lambda} = (0.830\,\mathrm{GeV})^2$. In addition, the initial values of the explicit chiral symmetry breaking strength and Yukawa coupling are $c = 2.82\times10^{-3}\,\mathrm{GeV}^3$ and $h_{k=\Lambda} = 10.18$. These parameters are fixed by fitting the vacuum physical observables, i.e., $f_\pi = 92\,\mathrm{MeV}$, $m_\psi = 300\,\mathrm{MeV}$, $m_\pi = 136\,\mathrm{MeV}$,and $m_\sigma = 479\,\mathrm{MeV}$.

The results we show in Fig. **??** is the kurtosis, i.e., the ratio of χ_4^B to χ_2^B, then the ratio of χ_6^B, χ_8^B to χ_2^B are given on the right. We use the kurtosis as a benchmark to fix our reduced temperature T_c^{glue} and α in the gluon potential and the rescale T_c of Fig. **??**. On the basis of a well tally of the kurtosis, the χ_6^B/χ_2^B and χ_8^B/χ_2^B are compared. We introduce a rescale temperature $T_c = 194$ MeV to remove the temperature difference between the lattice and the low energy effective model. We choose the T_c by fitting the kurtosis with the lattice results. We find that the value of T_c is related to the difference between the chiral phase transition temperature and confinement-deconfinement phase transition temperature. With the rising of the T_c^{glue} and α in the glue potential, the difference between chiral phase transition temperature and deconfinement phase transition temperature decreases at the same time the rescale T_c is rising. From the left diagram in the Fig. **??** we can clearly see, the FRG result is better match with the Wuppertal-Budapest Collaboration results, but a little higher than the HotQCD Collaboration results, especially around the $T/T_c = 0.9$ and $T/T_c = 1.2$. In another word, the FRG result has a slow change rate compared with HotQCD result.

The middle picture of Fig. **??** is the comparision of the χ_6^B/χ_2^B. The FRG result is better match with two lattice results at low and high temperature. However, the values of the FRG around $T/T_c = 1.0$ are not small enough to fit the lattice χ_6^B/χ_2^B. The valley depth of the FRG curve is related with the change rate of the kurtosis, i.e. the

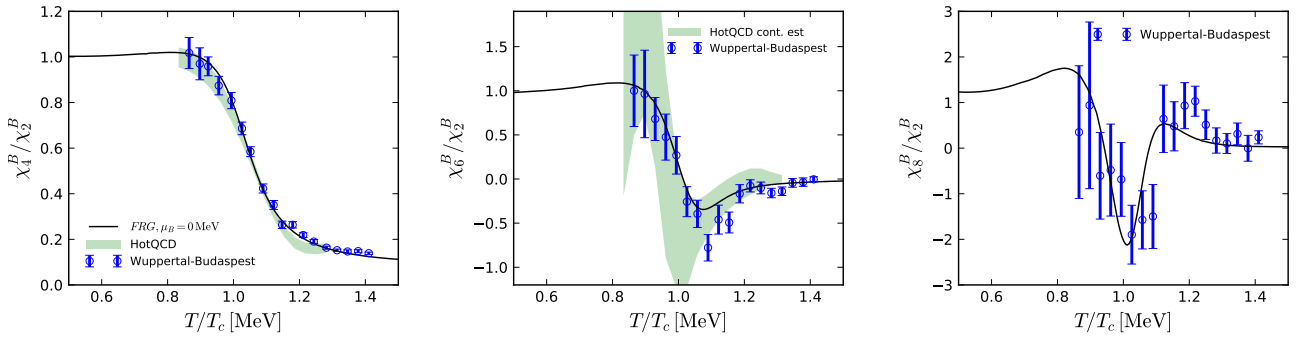

FIG. 1. χ_4^B/χ_2^B (left panel), χ_6^B/χ_2^B (middle panel), and χ_8^B/χ_2^B (right panel) as functions of the temperature with vanishing baryon chemical potential ($\mu_B = 0$). Results obtained with the low energy effective theory within the fRG approach are compared with those of lattice QCD, where the green bands show the extrapolated continuum value obtained from the HotQCD Collaboration [7, 8] and the blue dots show the results from the Wuppertal-Budapest Collaboration [9].

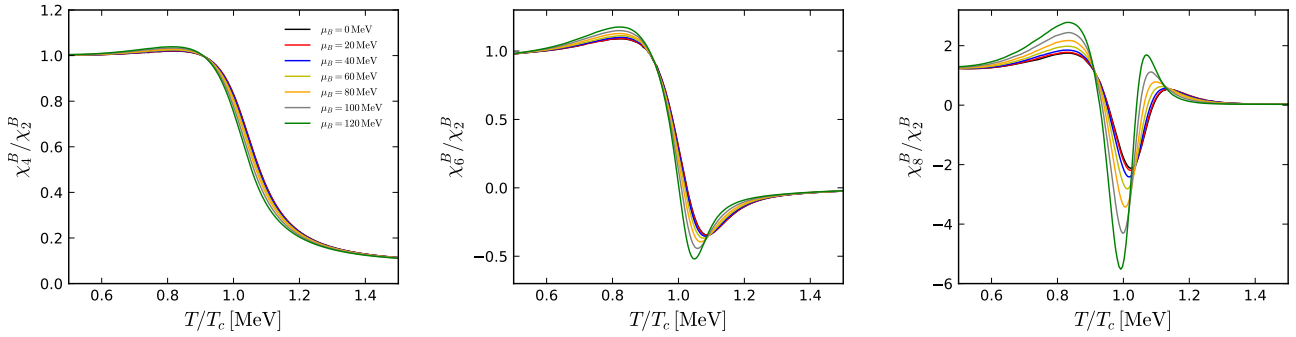

FIG. 2. χ_4^B/χ_2^B (left panel), χ_6^B/χ_2^B (middle panel), and χ_8^B/χ_2^B (right panel) as functions of the temperature with some selective values of μ_B from 0 to 120 MeV.

slow change rate of the kurtosis causes the shallow valley in the 6th order.

The last picture in Fig. **??** is the 8th order baryon number fluctuation. Here we only have the Wuppertal-Budapest Collaboration results. We can easily see from the picture, FRG is match well with lattice, except around $T/T_c = 1.2$, FRG curve is lower than the lattice. We believe the reason of the difference is also the slow change rate of the kurtosis.

The three pictures in Fig. 5 is the FRG results under finite baryon chemical potential from 0 to 400 MeV. As seen in left picture, the kurtosis grow high around $T/T_c = 0.8$ and become lower around $T/T_c = 0.95$. The behavior of the kurtosis under PQM model is also discussed in [10]. The change of the peak and valley values of the kurtosis lead to the slope change of kurtosis. So it is obvious that the 6th and 8th order fluctuations gradually increase to big values.

V. SUMMARY AND OUTLOOK

ACKNOWLEDGMENTS

The work was supported by the National Natural Science Foundation of China under Contracts Nos. 11775041.

[1] R. Wen, C. Huang, and W.-J. Fu, Phys. Rev. **D99**, 094019 (2019), arXiv:1809.04233 [hep-ph].
[2] C. Wetterich, Phys. Lett. **B301**, 90 (1993).
[3] S. Yin, R. Wen, and W.-j. Fu, (2019), arXiv:1907.10262 [hep-ph].
[4] P. M. Lo, B. Friman, O. Kaczmarek, K. Redlich, and C. Sasaki, Phys. Rev. **D88**, 074502 (2013), arXiv:1307.5958 [hep-lat].
[5] W.-j. Fu and J. M. Pawlowski, Phys. Rev. **D92**, 116006 (2015), arXiv:1508.06504 [hep-ph].
[6] J. M. Pawlowski and F. Rennecke, Phys. Rev. **D90**, 076002 (2014), arXiv:1403.1179 [hep-ph].
[7] A. Bazavov *et al.*, Phys. Rev. **D95**, 054504 (2017), arXiv:1701.04325 [hep-lat].

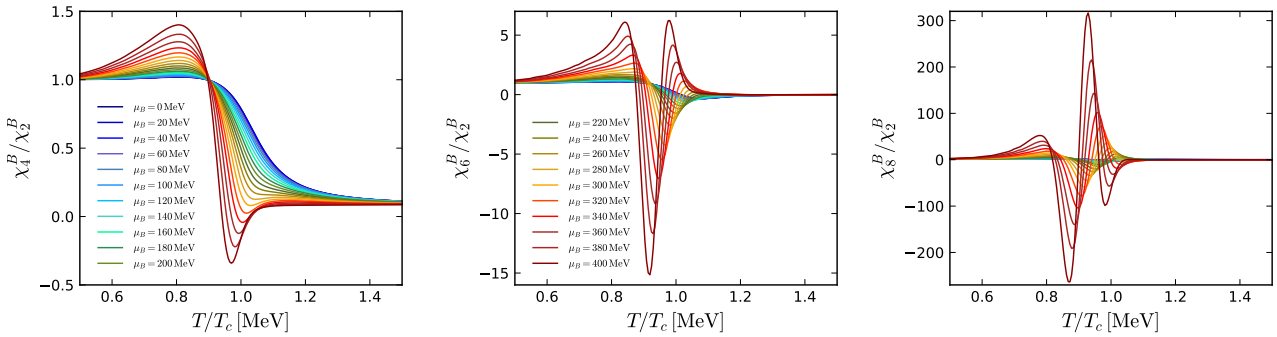

FIG. 3. Evolution of the dependence of χ_4^B/χ_2^B (left panel), χ_6^B/χ_2^B (middle panel), and χ_8^B/χ_2^B (right panel) on the temperature, with the increasing μ_B from 0 to 400 MeV.

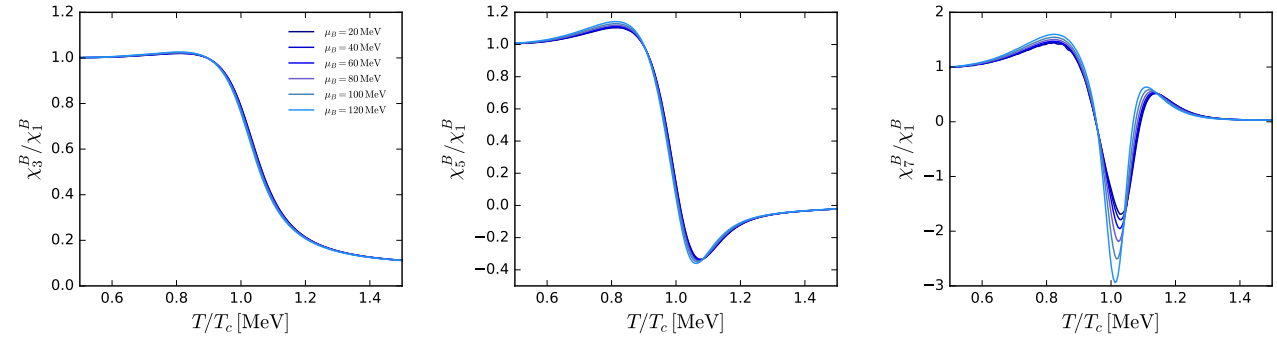

FIG. 4. χ_3^B/χ_1^B (left panel), χ_5^B/χ_1^B (middle panel), and χ_7^B/χ_1^B (right panel) as functions of the temperature with some selective values of μ_B from 0 to 120 MeV.

[8] A. Bazavov *et al.* (HotQCD), Phys. Rev. **D96**, 074510 (2017), arXiv:1708.04897 [hep-lat].

[9] S. Borsanyi, Z. Fodor, J. N. Guenther, S. K. Katz, K. K. Szabo, A. Pasztor, I. Portillo, and C. Ratti, JHEP **10**, 205 (2018), arXiv:1805.04445 [hep-lat].

[10] W.-j. Fu and J. M. Pawlowski, Phys. Rev. **D93**, 091501 (2016), arXiv:1512.08461 [hep-ph].

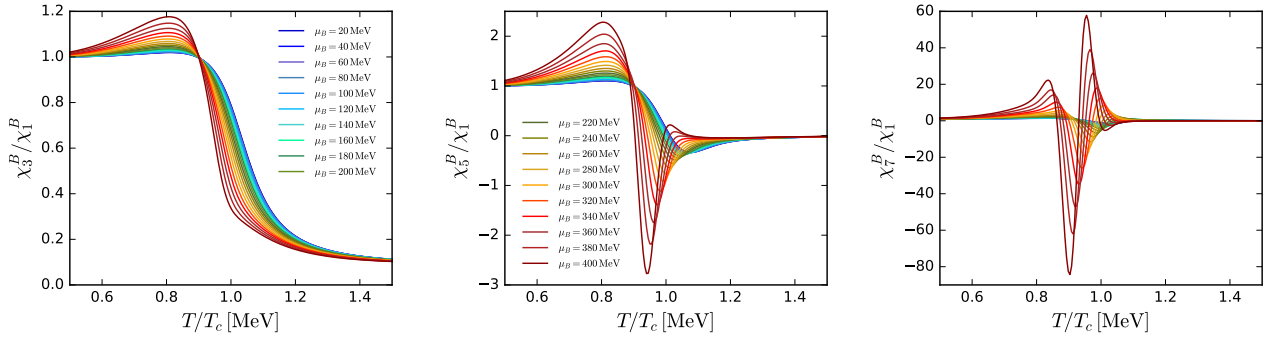

FIG. 5. Evolution of the dependence of χ_3^B/χ_1^B (left panel), χ_5^B/χ_1^B (middle panel), and χ_7^B/χ_1^B (right panel) on the temperature, with the increasing μ_B from 20 to 400 MeV.